Electronic Supplementary Material (ESI) for Physical Chemistry Chemical Physics.
This journal is © the Owner Societies 2018

Evolution in Graphitic Surface Wettability with First-Principles Quantum Simulations: The Counterintuitive Role of Water

*Jin-You Lu[1], Chia-Yun Lai[1], Ibraheem Almansoori[1], Matteo Chiesa[1]**

[1]Department of Mechanical and Materials Engineering, Masdar Institute,

Khalifa University of Science and Technology, P.O. Box 54224, Abu Dhabi, UAE

* Address correspondence to: matteo.chiesa@ku.ac.ae

Supporting Information

Contents

S.I Water/Graphite configurations

S.II Total energy of individual ice-like water layers on graphite surface

S. III Contact angle of water on graphite surface predicted by using van der Waals functional vdW-DF2

S.IV DFT AFM simulations on probing graphite and water/graphite surfaces

S. V Discussions on the Young-Dupre equation in terms of DFT-AFM predicted force of adhesion and adhesion energy

S.I Water/Graphite configurations

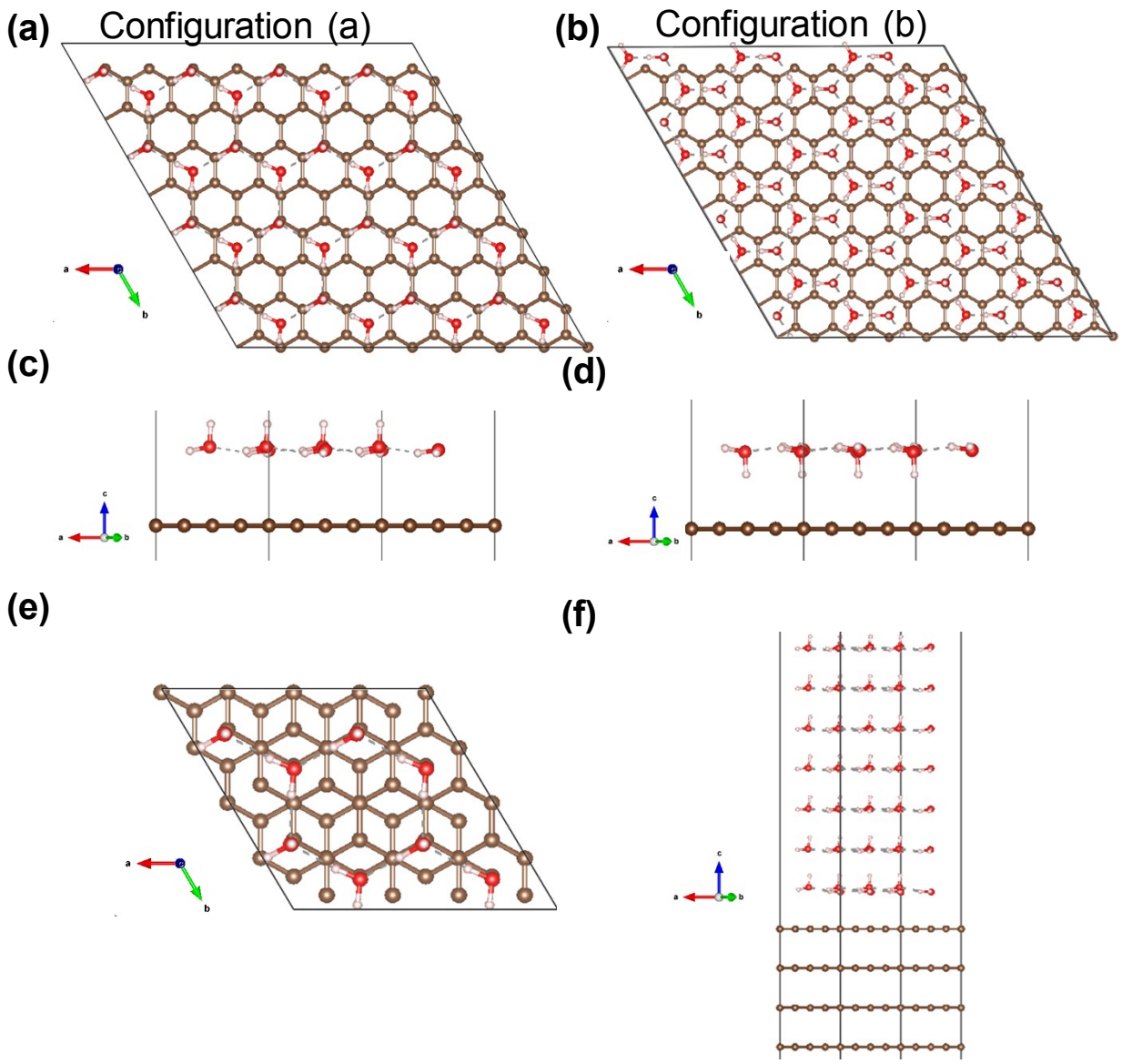

Figure S1. (a-b) Two possible configurations of a hexagonal ice structure on graphene surface, (c-d) OH-up and OH-down configurations of water structures on graphene surface (e-f) configuration used for the prediction of graphitic surface wettability in this work: Top and side views of relaxed water/graphite configuration.

we try several positions of a hexagonal ice structure on graphene surface, as indicated by experimental observations[1,2], before performing a series simulation of multiple water layers on graphite surface. Two possible positions of a hexagonal ice configuration on graphene surface are

shown in Fig. S1(a-b). Configuration-(a), corresponding to current used configuration in the manuscript, shows that some water molecules are situated on the center of graphene hexagons, and others are situated on top of carbon atoms. Configuration-(b) shows that all water molecules are situated on the center of graphene hexagons. Both configurations are stably relaxed through DFT geometry optimization; However, the configuration-(a) gives higher adsorption energy per water molecules (6. 29 kJ/mol) than that of configuration-(b) (4.92 kJ/mol). For the orientation of ice-like structure on the graphene surface, we found that the configuration (a) belongs to OH-up type, as shown in Fig. S1(c). An OH-down configuration in Fig. S1(d) is possibly existed, as indicated in ref.[3]. However, as we performed ab initio molecular dynamics on OH-down configuration, by using Berendsen ensemble. The water structure on graphene surface favors OH-up configuration. Therefore, the configuration we used is configuration (a) with OH-up water molecules. In the manuscript, the simulation supercell is a cuboids unit cell with primitive vectors of $\vec{A}=9.8448\hat{x}$ (Å), $\vec{B}=-4.9224\hat{x}+8.52585\hat{y}$ (Å), and $\vec{C}=70\hat{z}$ (Å). The interlayer distance between graphene layers is 3.34(Å), which match the experimental interlayer spacing in bulk graphite[4]. The average distance between the oxygen atoms of first ice-like water layer and graphite is 3.33(Å), which also agree with that predicted by other DFT simulations[5]. The average distance between two ice-like water layer is 3.42 (Å).

S.II total energy of individual ice-like water layers

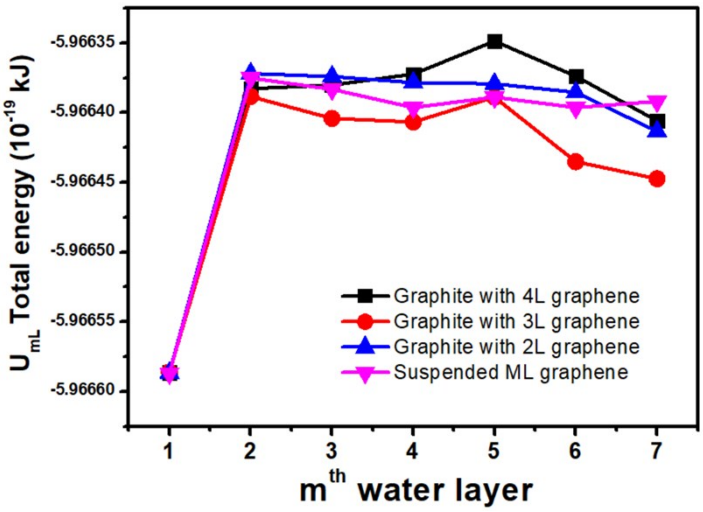

Figure S2. Total energy of the individual m^{th} water monolayer on different graphite surfaces.

For calculating the total energy of individual m^{th} water layer on graphite surface, the solid surface covered with $(m\text{-}1)^{th}$ water layers was removed from the relaxed water/graphite configurations. Then, the positions of water molecules in the individual m^{th} water layer were fixed to calculate its total energy. The DFT simulation results in Fig. S2 show that the first ice-like water layer is (lowest energy) most stable among all water layers, which agrees with the experimental observations.

S. III Contact angle of water on graphite surface predicted by using van der Waals functional vdW-DF2

In addition to using vdW-DF2-C09, we add the simulation results of water on graphite surface by using another van der Waals functional vdW-DF2[6] based on the same configurations used in the manuscript. Both adhesion U_{SL} and cohesion energy $U_{LV}/2$ are slightly larger than those obtained by using vdW-DF2-C09, and the simulation results shows as the number of graphite layer increases, the DFT-predicted contact angle decreases from 92.5+-2.1° (suspended graphene) to 86.65+-2.3° (four layers of graphene in a ABAB stacking). The graphite surface wettability predicted by both van der Waals functionals show similar trends; however, the graphite surface wettability predicted by using vdW-DF2 is more hydrophobic than that predicted by vdW-DF2-C09. This mismatch is probably owing to overestimation of hydrogen binding in vdW-DF2.

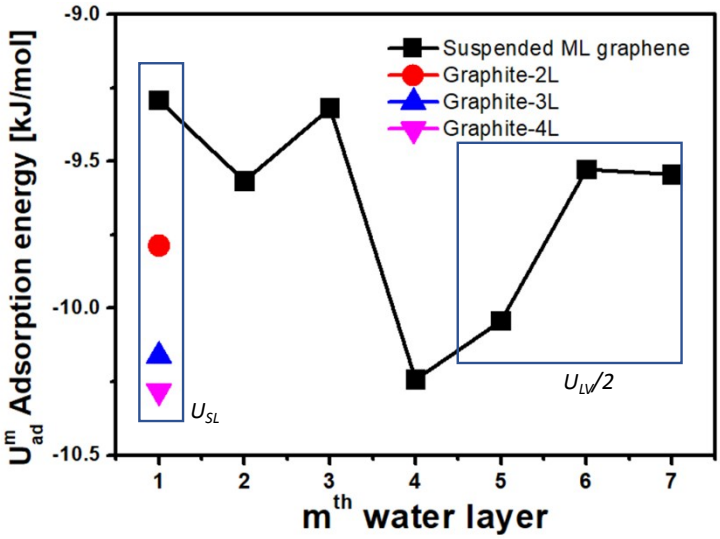

Figure S3. Adsorption energy per water molecule at different ice-like water layers on clean graphite surface predicted by using van der Waals functional vdW-DF2.

S. IV DFT AFM simulations on probing graphite and water/graphite surfaces

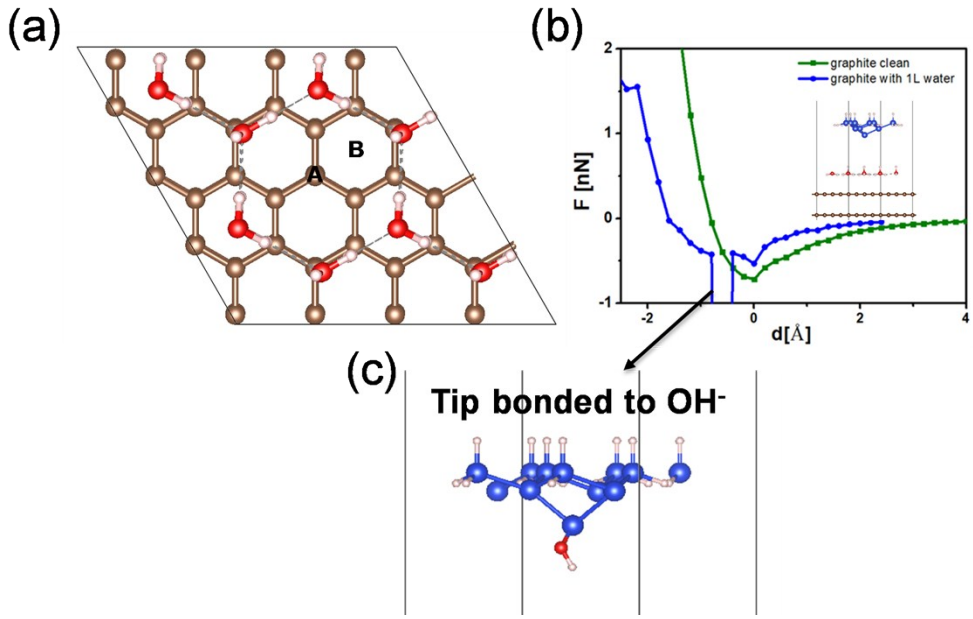

Figure S4(a) Two different probing points characterized by the DFT AFM simulations in this study. (b) DFT predicted force-distance curves of probing site B on graphite and water/graphite surfaces. (c) chemical reaction of O-H bonded to silicon tip occurring during the scanning.

In this study, the DFT-AFM simulations[78] are conducted to probe two different sites on graphite and graphite with one ice-like water layer from top to bottom in a quasi-static manner, and an interval of 0.2 Å. In Fig. S3(a), the site A and site B correspond to the position at the top of graphene's carbon atom and the center of graphene hexagon, respectively. The force-distance curves on site A of graphite and water/graphite surfaces are shown in the Fig.4 (a) of the manuscript. The force-distance curves on probing site B of the graphite and water/graphite surfaces in Fig. S4(b), have similar trends as those of probing site A except that the sudden drop owing to the chemical reaction of O-H bonded to the silicon tip, as shown in Fig. S4(c), happened at the different tip-to-surface distance. The reason for that is the position of the large attractive force drop

in the force-distance is dependent on the distance between the tip apex and nearest water molecules.

S. V Discussions on the Young-Dupre equation in terms of DFT-AFM predicted force of adhesion and adhesion energy

In order to link the surface wettability to the DFT-AFM simulations, we start with Young-Dupre equation, as shown in Eq. S1.

$$\cos(\theta) = \frac{W_{SL} - \gamma_{LV}}{\gamma_{LV}} \tag{S1}$$

Where W_{SL}, and R_{LV} are the work of adhesion at the solid/liquid interface and the surface tension at the liquid/vapor interface, respectively. These two physical quantities are equal to surface energy per unit area with the unit of J/m^2, as given by Eq. (S2).

$$\frac{W_{SL} - \gamma_{LV}}{\gamma_{LV}} = \frac{U_{SL}/A - U_{LV}/2A}{U_{LV}/2A} \tag{S2}$$

Where U_{SL} and U_{LV} are the surface energies at the solid/liquid and liquid/liquid interfaces, respectively. The surface areas A (or interaction area) at the solid/liquid and liquid/liquid interfaces are assumed to be same at the interface in the atomic scale. This assumption is tested by validating the calcite surfaces for different liquids[9], and the graphite surface for water liquid in this work. Then, the surface energy is calculated by the DFT adsorption (binding) energy studies[9].

$$\frac{U_{SL}/A - U_{LV}/2A}{U_{LV}/2A} = \frac{U_{ad,\,GW}/A - U_{ad,\,WW}/A}{U_{ad,\,WW}/A} \tag{S3}$$

Where $U_{ad,GW}$ is the adsorption energy of one water layer on graphite surface and $U_{ad,WW}$ is the adsorption energy of one water layer on water overlaying graphite surface. Basically, equation S3 is same as Eq. (1) in the manuscript. Then, we relate the Eq. (S3) to the minimal value of DFT-AFM adhesion energy in the energy-distance curve, as given by

$$\cos(\theta) = \frac{U_{ad,\,GW}/A - U_{ad,\,WW}/A}{U_{ad,\,WW}/A} \approx \frac{U_{GSi}/A - U_{WSi}/A}{U_{WSi}/A} = \frac{U_{GSi} - U_{WSi}}{U_{WSi}} \qquad \text{(S4)}$$

Where U_{GSi} and U_{WSi} are the adhesion (binding) energy between the silicon tip/graphite system and silicon tip/water system, respectively, as calculated by $U_{ad} = U(tip + surface) - U(tip) - U(surface)$. This is valid when the responses of water layer to clean graphite surface and water overlaying graphite surface are similar to those of silicon tip to clean graphite surface and water coved graphite. Actually, this concept is known and it comes from the idea of minimal value in the AFM Force-distance curve, which is the force of adhesion *Fad*. It gives the information of surface free energy on different surfaces by using a tip, as described by $F_{ad} = 4\pi R\gamma$ based on DMT model[10], where *R* is the tip radius. Meanwhile, since the force of adhesion F_{ad} is proportional to the surface energy per unit surface area as indicated by DMT model, we can also predict the surface wettability based on the DFT-AFM force of adhesion F_{ad}:

$$\cos(\theta) \approx \frac{U_{GSi}/A - U_{WSi}/A}{U_{WSi}/A} = \frac{F_{ad}^{G} - F_{ad}^{W/G}}{F_{ad}^{W/G}} \qquad \text{(S5)}$$

Where F_{ad}^{G} and $F_{ad}^{W/G}$ are the forces of adhesion on graphite and water/graphite surfaces, respectively.

We prefer using Eq. (S5) in predicting the surface wettability, which is able to have a direct comparison with the experimental AFM force-distance curve.

For the sake of completeness, the adhesion energy versus tip-to-surface distance is shown in the Fig. S5. The adhesion energy is calculated by the following equation: $U_{ad} = U(tip + surface) - U(tip) - U(surface)$, where *U* is the DFT calculated total energy. During the AFM scanning, the total energy of tip and surface are slightly changed in each step. Therefore, for calculating adhesion energy between the silicon tip and surfaces, the *U(tip)* and *U(surface)* are calculated, respectively, by using the configurations taken from the position where minimal of

adhesion energy occurs in Fig. S5. The origin of energy-distance curve is taken from position where the minimal of force-distance curve happened. By inputting the minimal values of energy-distance curve of graphite and water/graphite into the Eq. S4, the predicted contact angle is 73.3 ^{o}, which agree with the predicted contact angle of 72.3 ^{o} based on the forces of adhesion on these two surfaces, as summarized in Table S1. This agreement between contact angles predicted by AFM adhesion energy and AFM force of adhesion provides a self-consistent evidence of DFT-AFM numerical experiment.

Table S1. A comparison of contact angle prediction based on the DFT-AFM adhesion energy and DFT-AFM force of adhesion

Graphite surface	$F_{ad}^{graphite}$ (nN)	F_{ad}^{water} (nN)	Contact angle θ (^{o})	Experimental static contact angle (^{o})
DFT-AFM	-0.720	-0.552	72.3 ^{o}	68.2 ^{o} ± 1.6^{o}
Graphite surface	$U_{ad}^{graphite}$ (eV)	U_{ad}^{water} (eV)	Contact angle θ (^{o})	Experimental static contact angle (^{o})
DFT-AFM	-0.933	-0.724	73.3 ^{o}	68.2 ^{o} ± 1.6^{o}

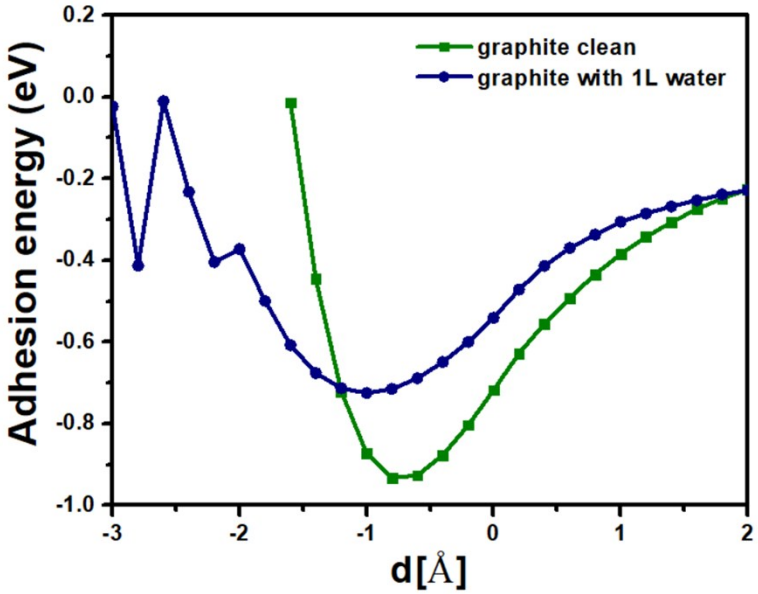

Figure S5. DFT predicted adhesion energy-distance curves on graphite and water/graphite surfaces.

Reference

(1) Xu, K.; Cao, P.; Heath, J. R.Graphene Visualizes the First Water Adlayers on Mica at Ambient Conditions. *Science (80-.).* **2010**, *329* (5996), 1188–1191.

(2) Teschke, O.Imaging Ice-like Structures Formed on HOPG at Room Temperature. *Langmuir* **2010**, *26* (22), 16986–16990.

(3) Ogasawara, H.; Brena, B.; Nordlund, D.; Nyberg, M.; Pelmenschikov, A.; Pettersson, L. G. M.; Nilsson, A.Structure and Bonding of Water on Pt (111). *Phys. Rev. Lett.* **2002**, *89* (27), 276102.

(4) Thanthiriwatte, K. S.; Hohenstein, E. G.; Burns, L. A.; Sherrill, C. D.Assessment of the Performance of DFT and DFT-D Methods for Describing Distance Dependence of Hydrogen-Bonded Interactions. *J. Chem. Theory Comput.* **2010**, *7* (1), 88–96.

(5) Sudiarta, I. W.; Geldart, D. J. W.Interaction Energy of a Water Molecule with a Single-Layer Graphitic Surface Modeled by Hydrogen-and Fluorine-Terminated Clusters. *J. Phys. Chem. A* **2006**, *110* (35), 10501–10506.

(6) Lee, K.; Murray, É. D.; Kong, L.; Lundqvist, B. I.; Langreth, D. C.Higher-Accuracy van Der Waals Density Functional. *Phys. Rev. B* **2010**, *82* (8), 81101.

(7) Huang, M.; Čuma, M.; Liu, F.Seeing the Atomic Orbital: First-Principles Study of the Effect of Tip Termination on Atomic Force Microscopy. *Phys. Rev. Lett.* **2003**, *90* (25), 256101.

(8) Caciuc, V.; Hölscher, H.; Blügel, S.; Fuchs, H.Atomic-Scale Sharpening of Silicon Tips in Noncontact Atomic Force Microscopy. *Phys. Rev. Lett.* **2006**, *96* (1), 16101.

(9) Lu, J. Y.; Ge, Q.; Li, H.; Raza, A.; Zhang, T.Direct Prediction of Calcite Surface Wettability with First-Principles Quantum Simulation. *J. Phys. Chem. Lett.* **2017**, *8* (21), 5309–5316.

(10) Derjaguin, B.V; Muller, V. M.; Toporov, Y. P.Effect of Contact Deformations on the Adhesion of Particles. *J. Colloid Interface Sci.* **1975**, *53* (2), 314–326.